第28卷第3期
2013年5月

热 能 动 力 工 程
JOURNAL OF ENGINEERING FOR THERMAL ENERGY AND POWER

Vol. 28, No. 3
May., 2013

文章编号: 1001-2060(2013)03-0292-04

非预混式旋流燃烧特性研究

王 凯,姜建国,关海滨,孙荣峰
(山东省科学院能源研究所,山东 济南 250014)

摘 要: 为计算非预混式旋流燃烧器的燃烧特性,建立了非预混强旋流燃烧过程模型,然后对两种不同结构形式的燃烧器进行了数值模拟,并在一个热态模型试验台上进行了相关燃烧试验,测量了热力参数并将参数与计算结果进行对比。结果表明: 采用两种燃烧器的燃烧室中高温区域都呈现双峰型分布,炉中心存在回流区域,此处轴向速度较小。燃烧器采用交叉与旋流相结合的形式比单纯采用旋流的形式,其气体燃烧速率更快,而且燃烧室中高温区域的体积更大、气流更均匀。试验结果与计算结果吻合较好,该方法可用于各种非预混燃气式燃烧器的燃烧计算。

关 键 词: 非预混,旋流燃烧器,数值模拟,热态试验

中图分类号: TK16; O242 文献标识码: A

引 言

非预混燃烧由于具有不回火、振动小、功率大、可预热到较高温度等优点,是目前大功率燃气燃烧器的主流燃烧方式。其强烈旋转的湍流扩散火焰结构也是未来燃烧器的发展方向之一。燃烧器性能直接决定了燃烧效率和设备运行可靠性。提高燃烧器的燃烧效率,对于提高热风温度、降低高炉焦比、节约焦炭能源、减少 CO 和 CO_2 气体的排放都有现实的指导意义[1]。

分层旋流燃烧是目前较常用的顶燃式热风炉的燃烧方式,它采用煤气在上层、空气在下层的非预混燃烧方式,国内学者对其燃烧器进行的理论分析表明[2-3],在燃烧器气体环道上各喷口配气较为均匀,在燃烧室出口气流分布也比较均匀,能够克服因气流分布不均造成的风温受限、蓄热砖下沉等缺陷,试验研究也证实采用该结构燃烧器的热风炉单烧高炉煤气(经过预热)时可提供 1 200 ℃的风温[4-5]。本研究针对一种新型燃烧器进行了燃烧性能的计算分析和试验研究,该燃烧器在原有分层旋流结构的基础上采用了空气、煤气喷口分层同排错列布置的方式,可使气流快速均匀的掺混燃烧,提高燃烧器的燃烧效率。

1 建立非预混旋流燃烧器的模型

1.1 燃烧器的结构

交叉分层旋流型燃烧器(以下称为 A 型)和分层旋流型燃烧器(以下称为 B 型)的结构示意图如图 1 所示。可以看出 A 型燃烧器的空气支管通过一个纵向的通道引出喷口,达到与上层的煤气喷口交错排列的目的,再加上气流喷口呈切向角布置的旋流作用,从而达到增加气流的接触面积和掺混速度,提高燃烧速率的效果。

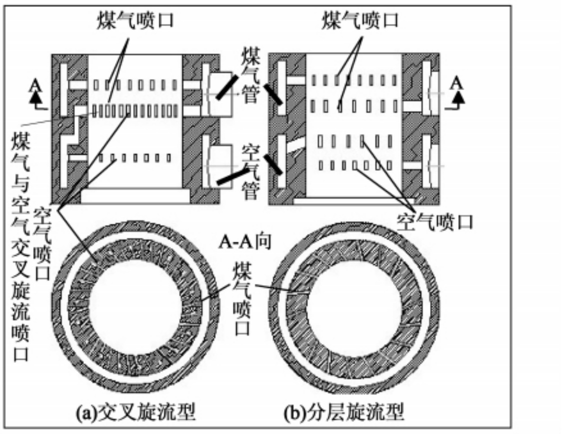

图1 两种燃烧器的结构
Fig. 1 Structure of two types of burner

1.2 物理模型

假设空气、煤气为牛顿型流体,且流动定常。由于燃烧过程处于高温,可假设混合气流为理想气体,则整个燃烧过程气体流动应满足连续方程、动量守恒和能量守恒方程。其控制方程为[6-7]:

$$\nabla \cdot (\rho \vec{v} \phi) = \nabla \cdot (\Gamma \nabla \phi) + S \qquad (1)$$

式中: ∇—散度; ρ—气体密度, kg/m^3; $\vec{v}$—速度矢

收稿日期:2012-08-03; 修订日期:2012-09-14
作者简介:王 凯(1982-),男,山东聊城人,山东省科学院副研究员

量,m/s; Φ—通用变量,Γ—广义扩散系数,S—广义源项,其具体表达式如表1所示。

表1　控制方程中各符号的表达式

Tab.1 Expression formulae of various signs in the control equation

	Φ	Γ	S
连续方程	1	0	0
动量守恒方程	$\vec{v}$	μ	$-\frac{\partial p}{\partial \vec{x}}+\rho\vec{g}$
能量守恒方程	T	λ/c_p	S_T

表1中:μ—动力粘度,N·s/m^2; p—气压,Pa; $\vec{x}$—坐标矢量; $\vec{g}$—重力加速度矢量,m/s^2; T—气温,K; λ—导热系数,W/(m·K); c_p—定压比热,J/(kg·K); S_T—粘性耗散项。炉内气流的燃烧采用非预混的PDF(混合分数概率密度函数)模型[8],其控制方程为:

$$\nabla\cdot(\rho\vec{v}\bar{f})=\nabla\cdot[(\mu_t/\sigma_t)\nabla\bar{f}] \quad (2)$$

$$\nabla\cdot(\rho\vec{v}\overline{f'^2})=\nabla\cdot[(\mu_t/\sigma_t)\nabla\overline{f'^2}]+C_g\mu_t(\nabla\bar{f})^2-C_d\rho(\varepsilon/k)\overline{f'^2} \quad (3)$$

式中:$f=(Z_i-Z_{i,ox})/(Z_{i,fuel}-Z_{i,ox})$,表示来源于煤气流元素的质量分数,用于求解燃烧过程的状态; $Z_{i,ox}$—空气流入口的元素i的质量分数; $Z_{i,fuel}$—煤气流入口的元素i的质量分数; k—流体的湍动能,m^2/s^2; ε—湍动能耗散率,m^2/s^3; μ_t—流体的湍动粘度,$\mu_t=\rho k^2/\varepsilon$,kg/(m·s); $\bar{f}$—f的时均值,$f'=f-\bar{f}$; 参数σ_t、C_g和C_d分别为0.85、2.86和2.0。热风炉内的辐射模型采用如下控制方程[8]:

$$\nabla\cdot\left(\frac{1}{3(a+\sigma_s)-C\sigma_s}\nabla G\right)=aG-4an^2\sigma_t T^4 \quad (4)$$

式中:G—入射辐射能,W; a—吸收系数; σ_s—散射系数; C—线性各向异性相位函数系数(取值范围-1~+1); n—折射指数; σ_t—Stefan-Boltzmann(斯蒂芬-波尔兹曼)常数(5.67×10^{-8} W/(m^2·K^4))。为使模型方程封闭,湍流模型采用标准$k-\varepsilon$模型[7]。

1.3　边界条件

热风炉计算模型区域如图2所示,其坐标原点取在炉底圆周的圆心,高度方向为z轴的正方向。其具体尺寸与热风炉的热态模型尺寸一致,模型总高4.5 m。截面1~截面9为从喉部至格子砖顶面的燃烧室空间内沿z轴负向排列的各个横切面。

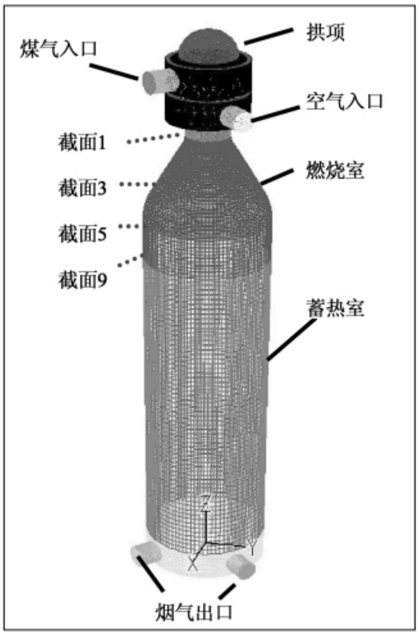

图2　计算模型区域的示意图

Fig.2 Schematic diagram of the zone calculated by using the model

热风炉的进口煤气成份采用高炉煤气,煤气和空气不预热,入口温度均为305 K。煤气支管和空气支管入口采用速度入口边界,入口速度分别为12.8和7.95 m/s。烟气出口采用压力出口边界,蓄热室格子砖采用多孔介质,其它边界面采用壁面边界。压力-速度耦合采用SIMPLEC(协调型压力耦合方程组的半隐式方法)算法求解,动量、能量等方程采用二阶迎风格式离散。

1.4　计算结果

图3给出了相同入口工况时,A型和B型燃烧器炉内温度场($x=0$截面)的对比结果。由图可知两种燃烧器燃烧室内的温度场分布规律略微相近,都呈现双峰型的高温区,只是在燃烧室内A型的高温区域体积要比B型的大,其燃烧温度也略高于B型。

图4给出了两种燃烧器炉内的CO气体浓度场($x=0$截面)对比结果,由图可知A型的CO燃烧效率更高,在燃烧室扩张段的中后段已经燃烧完毕;而B型燃烧器的炉内CO则是在扩张段的末段出口附近燃烧完毕。快速高效的燃烧使得A型的燃烧室

内高温区体积要大于 B 型的高温区。

两种燃烧器炉内气体的轴向速度对比如图 5 所示，其中纵坐标表示截面上某处的轴向速度，横坐标表示距离截面中心点的径向距离。可以看出两种燃烧器内气体的轴向速度分布规律类似，都呈现中心较低、随着径向距离增加而逐渐增大的趋势，在靠近壁面处由于边界层影响，速度又迅速减小。这表明强烈的旋流作用使炉中心产生了一个低压区，该区域内的气体产生回流，减小了炉中心气流的轴向速度。随着截面高度的逐渐降低，截面上各个点的速度分布逐渐趋向均匀。由图 5 还可知，A 型燃烧器炉燃烧室内各截面中心的轴向速度 v_z 略低于 B 型 v_z，壁面附近的 v_z 略高于 B 型 v_z，因此 A 型燃烧器的热风炉燃烧室内气流速度分布的均匀性要比 B 型好。

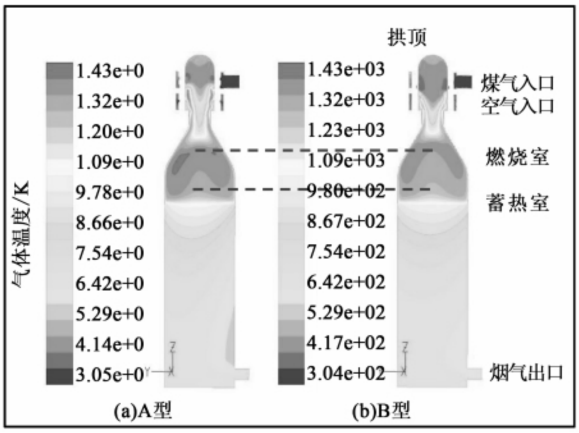

图 3 两种燃烧器炉内的温度场对比

Fig. 3 Comparison of the temperature fields inside the furnace using the two type of burner

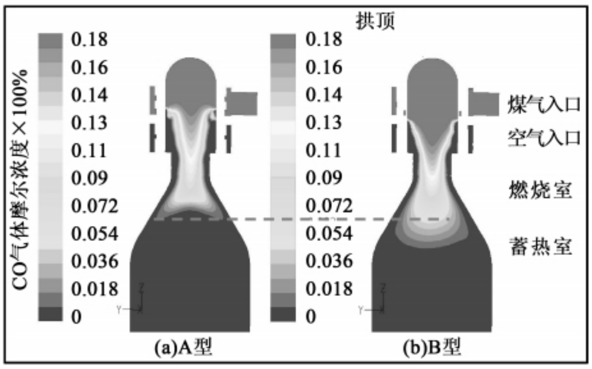

图 4 两种燃烧器炉内的 CO 气体浓度场对比

Fig. 4 Comparison of the CO gas concentration field inside the furnace using the two types of burner

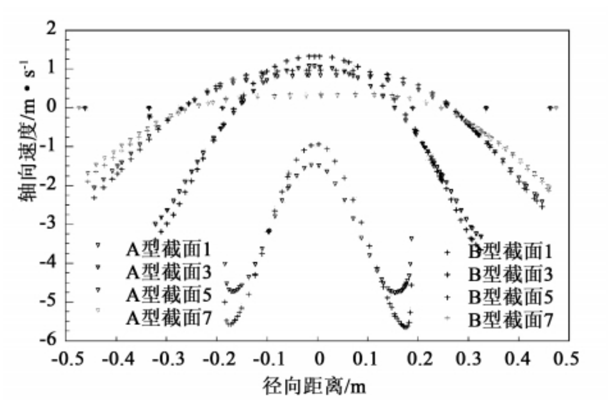

图 5 两种燃烧器炉内的轴向速度对比

Fig. 5 Comparison of the axial velocity inside the furnace using the two types of burner

2 实验验证及对比

2.1 试验流程

为了对模拟计算结果的可靠性进行分析，在 1∶10的模型试验台上进行燃烧实验，模型总高 4.5 m，内附耐热材料和蓄热砖，燃烧器采用 A 型结构。沿高度方向在热风炉上开若干测孔，用于测量各个截面混合气流燃烧时的浓度，每个截面间隔 50 mm 布置一个测点，浓度测试采用水冷取样管采集气体，用红外烟气分析仪进行分析。每个截面沿径向布置 2 个温度测点，温度采用瓷套管热电偶监测。

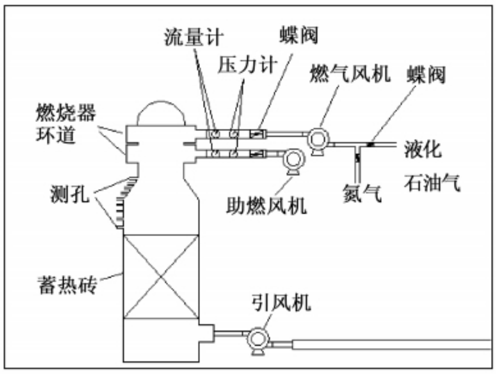

图 6 模型试验台结构

Fig. 6 Structure of the model test rig

图 6 给出了试验流程图，其燃料为工业氮气和液化石油气的混合气体，用以模仿高炉煤气的热值，燃气流和空气流依靠变频风机提供，可根据需要改变气体流量，燃气和空气压力均为 5 kPa。实验时的工况与模拟的入口条件基本相同。

2.2　结果对比

各个截面上测点平均温度的实测值与计算值的对比结果如图 7 所示，可以看出模拟结果基本反映了实测结果的变化规律，模拟值与实测值的相对误差小于 4%。

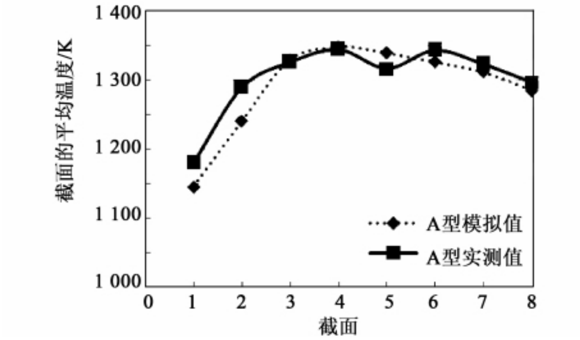

图 7　各个截面的平均温度比较

Fig. 7 Comparison of the average temperatures in various cross sections

图 8 为 A 型燃烧器炉燃烧室内的 CO 气体浓度的实测值与计算值的对比结果，由图可知模拟的浓度分布规律基本与实测结果相吻合。

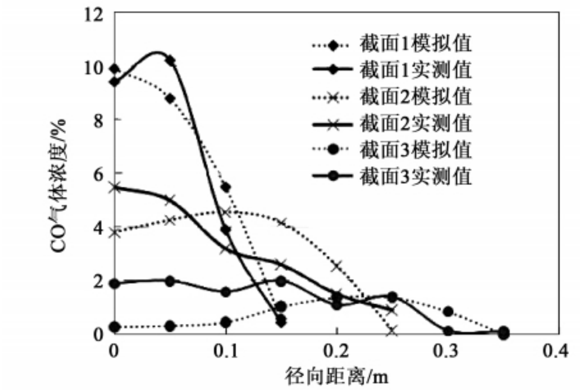

图 8　A 型燃烧器炉燃烧室内 CO 浓度比较

Fig. 8 Comparison of the CO concentrations inside the combustion chamber using type A burner

3　结　论

建立了非预混强旋流燃烧过程模型，然后对两种不同结构形式的燃烧器进行了模拟计算，并与热态模型试验的结果进行了对比。结果表明:

(1) A 型燃烧器因采用旋流技术和交错排列、分层布置的喷口形式，在相同的进气条件下，其炉内燃烧室的气流高温区域体积要比 B 型的大，而且气流的燃烧温度也高于 B 型; 两种燃烧器燃烧室内的高温区域都呈现双峰型分布。

(2) A 型燃烧器炉燃烧室内的 CO 气体燃烧速率比 B 型的高，在燃烧室扩张段的中后段就已经燃烧完毕。

(3) 两种燃烧器炉燃烧室内的气流速度分布规律类似，炉中心存在回流区，轴向速度较小。

(4) 模拟计算的结果与模型实测结果较为吻合，该方法可用于各种燃烧器形式的热风炉燃烧室内的燃烧计算。

参考文献:

[1] 饶荣水，戴方钦，王　立. 新型陶瓷燃烧器的模型实验研究[J]. 冶金能源，2001，20(2): 18-22.
RAO Rong-shui，DAI Fang-qin，WANG Li，Experimental Investigation of the model for new type ceramic burners [J]. Metallurgy & Energy Source，2001，20(2): 18-22.

[2] 张炳哲，张欣欣，于　帆，等. 卡卢金热风炉气体燃烧与流动数值模拟[J]. 工业炉，2005，27(6): 1-3.
ZHANG Bing-zhe，ZHANG Xin-xin，YU Fan，et al. Numerical simulation of the gas combustion and flow inside Kalugin hot blast furnace [J]. Industrial Furnace，2005，27(6): 1-3.

[3] 王标华，黄素逸，戴方钦. 顶燃式热风炉陶瓷燃烧器模型的数值模拟[J]. 冶金能源，2007，26(2): 24-27.
WANG Biao-hua，HUANG Su-yi，DAI Fang-qin. Numerical simulation of the model for ceramic burners in top-firing type hot-blast furnaces [J]. Metallurgy & Energy Source，2007，26(2): 24-27.

[4] 戴方钦，黄素逸，董　焰，等. 顶燃式热风炉多火孔无焰陶瓷燃烧器的研究与应用[J]. 钢铁，2007，42(11): 79-82.
DAI Fang-qin，HUANG Su-yi，DONG Yan，et al. Research and application of multi-port flameless ceramic burners in hot blast furnaces [J]. Iron & Steel，2007，42(11): 79-82.

[5] Dai fang-qin，Huang su-yi，Li shao-hua，et al. Study of a ceramic burner for shaftless stoves [J]. International journal of minerals，metallurgy and materials，2009，16(2): 149-153.

[6] 王福军. 计算流体动力学分析—CFD 软件原理与应用[M]. 北京: 清华大学出版社，2004.
WANG Fu-jun. Computational fluid dynamic analysis-CFD software principle and applications [M]. Beijing: Tshing-hua University Press: 2004.

[7] 陶文铨，数值传热学[M]. 西安: 西安交通大学出版社，2004.
TAO Wen-quan. Numerical heat transfer [M]. Xián: Xián Jiaotong University Press: 2004.

[8] ANSYS FLUENT 12.0 Theory Guide [R]，ANSYS，Inc: 2009.

(陈　滨　编辑)

desulfurization, aerosol, process parameter, influence

干式排渣机锅炉烟风系统设计优化方法 = Optimization Methods for Designing the Flue Gas and Air System of a Boiler [刊,汉] LU Ming, LI Shuang-jiang (Hebei Electric Power Prospecting and Designing Research Institute, Shijiazhuang, China, Post Code: 050031) //Journal of Engineering for Thermal Energy & Power. -2013, 28(3). -288~291

At present, for a unit using a dry slag discharging system, the excessive air leakage of the dry slag discharging system is not counted in the traditional design and calculation of the flue gas and air system, causing the efficiency of the boiler being lowered during its actual operation and the capacity of the forced draft fan chosen being excessively large. To this end, a method for designing and optimizing flue gas and air systems to overcome this problem was presented. On the basis of the traditional calculation of flue gas and air systems, the influence of the unorganized air leakage of the dry slag discharging system on the boiler efficiency was quantitatively analyzed. Through an optimization of the design method, the unorganized air leakage of the dry slag discharging system can be counted in the calculation of the flue gas and air system of the boiler, offering guidnce in selecting the capacity of the air preheater in advance to reduce the flue gas losses of the boiler and guarantee the boiler efficiency. In the meantime, the air quantity of the forced draft fan of the boiler can be determined more rationally and the parameters of the forced draft fan can be lowered, thus reducing the manufacturing cost and enhancing the operation cost-effectiveness. Through applications in the actual engineering projects, 8 800 tons of coal can be saved in each year for a single unit with expenses of RMB 44 million yuan being avoided and for each unit, electric power of 797 500 kWh and expenses of RMB 398750 yuan can be saved annually. **Key words:** dry slag discharging, boiler air leakage, energy saving and emissions reduction, air preheater, forced draft fan

非预混式旋流燃烧特性研究 = Study of the Non-premixed Type Swirling Combustion Characteristics [刊,汉] WANG Kai, JIANG Jian-guo, GUAN Hai-bin, SUN Rong-feng (Energy Source Research Institute, Shandong Provincial Academy of Sciences, Jinan, China, Post Code: 250014) //Journal of Engineering for Thermal Energy & Power. -2013, 28(3). -292~295

Established was a mathematical model for calculating the combustion characteristics of a non-premixed type swirling burner and then, numerically simulated were two burners with different structures with relevant combustion tests being conducted on a hot-state model test rig and the thermal parameters being measured and compared with the calculation results. The research results show that the high temperature zones in the combustion chamber of both burners all assume a dual peak type distribution and there exist return flow zones in the center of the furnaces where the

axial speed is relatively small. The gas combustion speed of the burner with a structure integrating a cross flow and a swirling one will be quicker than that with a structure adopting a single swirling flow and the high temperature zone in the combustion chamber will have a larger volume and an even more uniform flow. The test results are in relatively good agreement with the calculation ones. The method under discussion can be used for calculating the combustion of various non-premixed type burners. **Key words:** non-premixed, swirling burner, numerical simulation, hot-state test

扇形腔多油垫静压推力轴承润滑性能速度特性 = Lubrication Performance and Velocity Characteristics of a Multi-oil-pad Hydrostatic Thrust Bearing with a Sector-shaped Cavity [刊,汉] YU Xiao-dong, QIU Zhi-xin, LI Huan-huan, TAN Li (College of Mechanical and Power Engineering, Harbin University of Science and Technology, Harbin, China, Post Code: 150080) // Journal of Engineering for Thermal Energy & Power. -2013, 28(3). -296 ~300

The lubrication performance of a multi-oil-pad hydrostatic thrust bearing with a sector cavity is conspicuously influenced by the velocity and if it is designed improperly, the lubricating oil film may be fractured and dry friction may result and if worsened, the hydrostatic bearing may fail due to friction. In the light of such a problem, the fluid dynamics and lubrication theory were applied to numerically analyze the velocity characteristics of such parameters as the pressure, flow rate and oil film thickness in the oil cavity etc. As a result, the law of the velocity influencing the lubrication parameters of the multi-oil-pad hydrostatic thrust bearing with a sector-shaped cavity was obtained, thus making it possible to avoid the occurrence of such a failure. The research results show that with an increase of the rotating speed of the rotary work bench, the lubricating oil flow rate caused by the action of both inertia force and centrifugal force will also increase, therefore the oil flow rate going out from the oil cavity will increase and the pressure in the cavity will drop, resulting in a thinner oil film thickness and fracture of the oil film and causing dry friction with a failure of the hydrostatic bearing due to friction. The foregoing can offer basic data for design, lubrication and tests of a hydrostatic thrust bearing and realize a prediction of its lubrication performance and velocity characteristics, thus attaining the aim of reducing the economic losses. **Key words:** velocity characteristics, sector-shaped cavity multi-oil-pad, hydrostatic thrust bearing, lubrication performance

电站锅炉汽动引风机排汽接除氧器的热经济性分析 = Analysis of the Thermal Cost-effectiveness of the Exhaust Steam of the Steam-driven Induced Draft Fan of a Utility Boiler When Introduced into Deaerators [刊,汉] YANG Yan-ling, SHI Qi-guang, JIN Rong, ZHAI Shu-wei (College of Energy Source and Environment Engineering, Shanghai College of Electric Power, Shanghai, China, Post Code: 200090) //Journal of Engineering for